International Journal of Applied Science and Engineering
2003. 1, 1: 1-16

Prediction of Dispersion Relation for Elastic Stress Waves in Prestressed Tendons Using 1-D Member Theories

Chih-Peng Yu* and Chih-Hung Chiang

Department of Construction Engineering, Chaoyang University of Technology, Wufeng, Taichung County 413, Taiwan, R.O.C.

Abstract: The analytical determination of dispersion relations of stress waves propagating within an axisymmetric member has been well established during the past four or five decades. For dynamic analysis associated with fundamental modes of vibration, various one-dimensional (1-D) member theories have been proven to be able to reproduce reasonable approximations for the dispersion relationship. These 1-D member theories provide more efficient and simpler solutions than those obtained by the three-dimensional (3-D) elasticity theory since the need for evaluating special functions such as Bessel functions is eliminated. To assess the loss in prestressing force, elastic waves were applied by various researchers to slender members of axisymmetric cross sections, such as seven-wire-strand tendons and underground pipelines. Thus the feasibility of using the 1-D member theories to predict the associated dispersion phenomenon should be addressed. In this work, formulations of most applicable 1-D linear theories were summarized and corresponding dispersion approximations were obtained in terms of dimensionless parameters. These formulations include the three-mode Mindlin-McNiven theory for axial vibrations, the two-mode Timoshenko beam theory for transverse vibrations, and the nonlinear theory for cable dynamics.

Keywords: dispersion; stress waves; prestressing members.

1. Introduction

Wave mechanics associated with slender members of axisymmetric cross sections has been well studied some fifty to sixty years ago. Although exact formulations for certain simple cases had been derived as early as in the late nineteenth century, the complicated nature of the exact solutions of these 3-D formulations limited their applications to engineering problems until the advent of the era of modern numerical computations. On the other hand, approximations using simpler 1-D theories were widely accepted in the dynamic analysis of rod-like members even before the computer age. At the present time, the 1-D theories are still efficient in providing reasonable solutions to the fundamental modes of vibration and wave propagation. For slender members under the action of prestressing forces, the derivation of the exact 3-D formulations may not be possible while the 1-D linear theories can still take into account the prestressing effect by approximation. Nevertheless, it is intended in this paper to incorporate the effect of axial loads into the 1-D linear theories and to study possible variations of the dispersion characteristics associated with the prestressed members.

The dynamic formulations for various 1-D linear members, such as a rod, a cable, and a beam or a beam-column, have been ex-

* Corresponding author: E-mail: cpyu@mail.cyut.edu.tw *Accepted for Publication: Dec. 28, 2002*

tensively investigated. As far as the elastic dispersion relation is concerned, these 1-D formulations normally lead to predictions in good agreement with those obtained from the 3-D ones. During the past fifty years, many researchers have developed useful 1-D approximation theories and proposed valuable applications to specific engineering problems. For example, a relatively rigorous formulation associated with the axial vibration of rods was derived as early as 1951 by Mindlin and Herrmann [1] and were proven to be practically correct in predicting the dispersion curves for the first two modes of the axial wave propagation. Mindlin and McNiven [2] later extended this work to further include second order axial deformation in the formulation. Through the use of certain combinations of the so-called adjustment coefficients, the corresponding predictions of the dispersion curves match quite well with the 3-D solutions, particularly for the first-mode longitudinal wave.

A well-known approximation for the flexural behavior of beams, recognized as the Timoshenko beam theory, has been widely adopted in both static and dynamic analyses of structures, particularly for deep beams. Dynamic analysis using such a theory results in very good predictions for the first two modes of the flexural wave propagation. Based on this approximation theory, more general forms considering the effects due to the axial force and distributed restraints were proposed and applied to dynamic problems associated with axially loaded member. Chen et al conducted a comprehensive study of the dynamic response of an axially loaded beam on a viscoelastic foundation using a continuous dynamic stiffness formulation based on the Timoshenko beam theory [3]. Yu & Roësset used continuous formulations to carry out a series of studies on various dynamic problems associated with seismic response as well as non-destructive dynamic testing of structural elements [4-6].

Dynamic behavior of tensioned cables is usually described by the classical cable theory that neglects the second order displacements and the inertial effect in the axial direction. This simple approximation leads to a non-dispersive relation associated with the transverse vibration of the tensioned cable. Sarkar & Manohar proposed a rather comprehensive model regarding the continuous dynamic formulations for a tensioned cable with a quadratic geometric profile and subjected to a constantly moving axial load [7]. Such formulation results in two dispersion branches with respect to both the transverse and axial vibrations.

For members with uniform sectional properties, the exact solutions based on the corresponding 1-D theories can usually be expressed in terms of exponential functions and thus the derivation of the dispersion formulae is straightforward. Similar derivation seems impossible for non-uniform members such as a seven-wire strand. Only 1-D approximation may be obtained for a specific wire in such a sophisticated configuration. Instead of attempting to derive the exact formulation for non-uniform members, approximations based on solutions for curved beams can be used to provide dispersion information for the outer spiral wires. This approach provides often better approximations than the traditional estimation using the straight-member solutions. In this paper we concentrate however on straight members of uniform cross sectional properties. Various formulations are considered, including an axial member under axial deformation, a beam under axial load, and a cable-like member under both axial (prestressing) and lateral (dead) loads. Modifications of the second order theory for axial members are made to incorporate the confining effect due to the peripheral tractions. Such modifications provide an efficient way to evaluate the dispersion relation of the center wire of a seven-wire strand by avoiding some additional computations.

2. Formulations for axially loaded members

2.1. Mindlin-McNiven theory for rod

In this second order theory, three nodal degrees of freedom are used to represent the first order uniform axial deformation u_1, the linearly varying lateral contraction u_c, and the second order quadratic axial deformation u_2, respectively. Following the derivation proposed by Mindlin and McNiven [2], the governing equations of a uniform rod with a circular cross section of radius a can be shown as

$$\mu k_2^2(a^2\psi'' - 4w') - 8(\lambda+\mu)k_1^2\psi - 4\lambda k_1 u' + 4R = \rho a^2 k_3^2 \ddot{\psi} \tag{1a}$$

$$2a^2\lambda k_1\psi' + a^2(\lambda+2\mu)u'' + 2aZ = \rho a^2 \ddot{u} \tag{1b}$$

$$a^2(\lambda+2\mu)w'' + 6\mu k_2^2(a^2\psi' - 4w) - 6aZ = \rho a^2 k_4^2 \ddot{w} \tag{1c}$$

where λ and μ are the Lame's constants, ρ is the mass density, R and Z are the distributed peripheral stresses in the radial and longitudinal directions, respectively. The adjustment factors k_i's are intended to make the spectral characteristics match the comparable dispersion curves from the exact 3-D theory. In these equations, the three deformation variables, u_1, u_c, and u_2, have been expressed in terms of the uniform first-order axial displacement u, the constant lateral contraction strain ψ, and the second-order axial deformation w, respectively, as

$$u_1 = u$$
$$u_c = a\psi$$
$$u_2 = \left[1 - 2\left(\tfrac{r}{a}\right)^2\right]w$$

Integrating the above stress equations over the circular cross section, the equations of motion can be expressed in terms of the member forces with respect to natural boundary conditions as

$$\frac{\partial Q}{\partial x} - P_r + 2AR = k_3^2 \rho I_P \ddot{\psi} \tag{2a}$$

$$\frac{\partial F}{\partial x} + 2\pi a Z = \rho A \ddot{u} \tag{2b}$$

$$3\left(\frac{\partial F_1}{\partial x}\right) + 12\left(\frac{Q}{a^2}\right) - 6\pi a Z = k_4^2 \rho A \ddot{w} \tag{2c}$$

where F and Q are the axial force and lateral contraction moment, respectively. P_r is the resultant internal force integrated from the stress components in the radial and transverse directions. F_1 is the integration of the quadratic distributed axial force associated with the second order axial deformation. These forces can also be expressed as

$$F = 2k_1\lambda A\psi + (\lambda+2\mu)Au' \tag{3}$$

$$Q = k_2^2 \mu I_P \psi' - 2k_2^2 \mu A w \tag{4}$$

$$F_1 = \tfrac{1}{3}(\lambda+2\mu)Aw' \tag{5}$$

$$P_r = 4k_1^2(\lambda+\mu)A\psi + 2k_1\lambda A u' \tag{6}$$

By neglecting R and Z and converting all equations to the frequency domain, the spectral equations of motion become

$$k_2^2\mu I_P\hat{\psi}'' - 2k_2^2\mu A\hat{w}' - 4k_1^2(\lambda+\mu)A\hat{\psi} - 2k_1\lambda A\hat{u}' = -(k_3^2\rho I_P\omega^2)\hat{\psi} = -D_c\hat{\psi} \tag{7a}$$

$$2k_1\lambda A\hat{\psi}' + (\lambda+2\mu)A\hat{u}'' = -(\rho A\omega^2)\hat{u} = -D_x\hat{u} \tag{7b}$$

$$(\lambda+2\mu)A\hat{w}'' + 6k_2^2\mu A\hat{\psi}' - 24k_2^2\mu\pi\hat{w} = -(k_4^2\rho A\omega^2)\hat{w} = -D_s\hat{w} \tag{7c}$$

where

$D_c = (k_3^2 \omega^2 \rho I_P)$

$D_x = (\omega^2 \rho A)$

$D_s = (k_4^2 \omega^2 \rho A)$.

The governing equations of the three-mode model can be obtained by expressing Eq. (7a) to (7c) in the matrix form.

Assume the solutions to this system of ordinary second-order differential equations for the three displacements to be

$$\widehat{u} = \sum_{j=1}^{6} C_j e^{\bar{r}_j x} \tag{8a}$$

$$\widehat{\psi} = \sum_{j=1}^{6} D_j e^{\bar{r}_j x} = \sum_{j=1}^{6} \overline{K}_j C_j e^{\bar{r}_j x} \tag{8b}$$

$$\widehat{w} = \sum_{j=1}^{6} E_j e^{\bar{r}_j x} = \sum_{j=1}^{6} \overline{L}_j C_j e^{\bar{r}_j x} \tag{8c}$$

Substitution of these solutions into Eqs. (7a) to (7c) leads to,

$$\begin{bmatrix} (\lambda+2\mu)A\bar{r}^2 + D_x & 2k_1\lambda A\bar{r} & \\ -2k_1\lambda A\bar{r} & k_2^2\mu I_P\bar{r}^2 - 4k_1^2(\lambda+\mu)A + D_c & -2k_2^2\mu A\bar{r} \\ & 2k_2^2\mu A\bar{r} & \frac{1}{3}\left((\lambda+2\mu)A\bar{r}^2 - 24k_2^2\mu\pi + D_s\right) \end{bmatrix} \begin{Bmatrix} \widehat{u} \\ \widehat{\psi} \\ \widehat{w} \end{Bmatrix} \tag{9}$$

$$= \left[\widehat{\mathbf{S}}\right]\left\{\widehat{U}\right\} = 0$$

The spectral characteristic equations of this three-mode model can thus be obtained by expanding the determinant of the frequency dependent matrix $\widehat{\mathbf{S}}$ as

$$a_3\bar{r}^6 + a_2\bar{r}^4 + a_1\bar{r}^2 + a_0 = 0 \tag{10}$$

The constants are

$a_3 = cg^2$,

$a_2 = cg(D_1 + D_3) + gh_1$,

$a_1 = h_1h_3 + gh_2D_1 + cD_1D_3$,

$a_0 = h_2h_3D_1$

with the following symbols

$D_1 = D_x$

$D_2 = D_c$

$D_3 = D_s$

$h_1 = D_2g - 4k_1^2EqA^2$

$h_2 = D_2 - 4k_1^2qA$

$h_3 = D_3 - 24k_2^2f$

$c = k_2^2\mu I_P$

$f = \mu\pi$

$g = (\lambda + 2\mu)A$

$q = (\lambda + \mu)$

Eq. (10) is a cubic equation with respect to $\bar{r}^2$. The three roots of $\bar{r}^2$ can be obtained either numerically or analytically from explicit expressions of a cubic equation as shown in reference [9]. The dispersion curves can thus be derived from the relation between the characteristic root and the frequency in which the imaginary part of the characteristic root represents the wave number of the propagating wave.

Next we consider the application of this theory to the modeling of the center wire of a seven-wire strand. The confining effect from the 6 spiral wires can be taken into account assuming that both the confining and frictional forces are uniformly distributed in the form of the equivalent peripheral stresses *R* and *Z*. Although Eq. (2) allows the inclusion

of peripheral stresses, only stresses as functions of the three displacements will result in changes of the characteristic Eq. (10) and thus lead to different dispersion curves. Assuming these confining and frictional forces to be distributed restraints along the center wire, the integrated peripheral forces can be expressed in a simple form as

$$2\pi a\hat{Z} = y_1\hat{u} + y_2\hat{w} \tag{11}$$

in which the coefficients y_i's depend on the geometry of the peripheral wires and the axial force.

In Eq. (11), the confining effect is simply interpreted as functions of the two axial displacements. This assumption seems reasonable since different levels of the confining stresses in the centrifugal direction cause different restraining effects on the center wire and the radial stresses depend actually on the magnitudes of the axial forces in the peripheral wires. Substitute Eq. (11) into Eqs. (1a) to (1c), the revised version of Eq. (9) can be shown as

$$\begin{bmatrix} (\lambda+2\mu)Ar^2 + D_x + y_1 & 2k_1\lambda Ar & +y_2 \\ -2k_1\lambda Ar & k_2^2\mu I_P r^2 - 4k_1^2(\lambda+\mu)A + D_c & -2k_2^2\mu Ar \\ -y_1 & 2k_2^2\mu Ar & \frac{1}{3}\left((\lambda+2\mu)Ar^2 - 24k_2^2\mu\pi + D_s\right) - y_2 \end{bmatrix} \begin{Bmatrix} \hat{u} \\ \hat{\psi} \\ \hat{w} \end{Bmatrix} = 0 \tag{12}$$

An approximate dispersion relation for the center wire can then be obtained from solving the characteristic equation associated with Eq. (12). It is noted that Eq. (2) may also be used to provide approximate characteristic equations for various dynamic problems associated with the axial deformation of straight members as long as the peripheral stresses can be manipulatively correlated with the displacement functions.

2.2. General theory for beam

Next we consider the traditional Timoshenko beam theory with additional assumptions for the axial force and distributed restraints. The governing equation for a general flexural member under the action of axial force can be shown as

$$\left(1+\tfrac{N}{\kappa GA}\right)EI\hat{v}^{IV} + \left(\tfrac{EI}{\kappa GA}D_f - \left(1+\tfrac{N}{EA}\right)N + \left(1+\tfrac{N}{\kappa GA}\right)D_r\right)\hat{v}'' - D_f\left(\left(1+\tfrac{N}{EA}\right) - \tfrac{D_r}{\kappa GA}\right)\hat{v} = 0 \tag{13a}$$

or

$$\hat{v}^{IV} + \left(\frac{1}{\left(1+\frac{N}{\kappa GA}\right)}\frac{D_f}{\kappa GA} - \frac{\left(1+\frac{N}{EA}\right)}{\left(1+\frac{N}{\kappa GA}\right)}\frac{N}{EI} + \frac{D_r}{EI}\right)\hat{v}'' - \frac{1}{\left(1+\frac{N}{\kappa GA}\right)}\frac{D_f}{EI}\left(\left(1+\tfrac{N}{EA}\right) - \tfrac{D_r}{\kappa GA}\right)\hat{v} = 0 \tag{13b}$$

where N represents axial force (positive for tension), κ is the shear coefficient of the cross section, and two spectral constants are introduced to simply the expression, namely $D_r = \rho I\omega^2$ and $D_f = \rho A\omega^2$.

Substitution of the following solution,

$$\hat{v} = \sum_{j=1}^{4} C_j e^{\bar{r}_j x} \tag{14}$$

gives a characteristic equation in the form as

$$\bar{r}^4 + 2\beta\bar{r}^2 - \alpha^2 = 0 \tag{15}$$

where $2\beta = \frac{D_f}{(\kappa GA+N)} - \frac{\left(1+\frac{N}{EA}\right)}{\left(1+\frac{N}{\kappa GA}\right)}\frac{N}{EI} + \frac{D_r}{EI}$

and $\alpha^2 = \frac{D_f}{\left(1+\frac{N}{\kappa GA}\right)EI}\left(\left(1+\frac{N}{EA}\right) - \frac{D_r}{\kappa GA}\right)$.

Normally, the effects of *N/EA* and *N/GA* are so small that the governing differential equation can be reduced to

$$EI\hat{v}^{IV} + \left[\frac{EI}{\kappa GA}D_f - N + D_r\right]\hat{v}'' - D_f\left[1 - \frac{D_r}{\kappa GA}\right]\hat{v} = 0 \tag{16}$$

Therefore, the coefficients for the characteristic equation can be expressed as

$$2\beta = \left(\frac{D_f}{\kappa GA} - \frac{N}{EI}\right) + \frac{D_r}{EI}$$
$$\alpha^2 = \left(\frac{D_f}{EI}(1 - \frac{D_r}{\kappa GA})\right) \tag{17}$$

The corresponding dispersion curves can then be computed by solving the characteristic root with

$$\overline{r_j}^2 = -\beta \pm \sqrt{\beta^2 + \alpha^2}$$

2.3. General theory for cable

According to Sarkar & Manohar [7], the governing differential equations for a vibrating cable taking into account the coupling effect between axial and transverse deformations are given as

$$\frac{\partial}{\partial x}\left[\mathrm{P}(x)\frac{\partial v}{\partial x} + \mathrm{EA}(x)\left(\frac{dy}{dx}\right)\frac{\partial u}{\partial x} + \mathrm{EA}(x)\left(\frac{dy}{dx}\right)^2\frac{\partial v}{\partial x}\right] = \frac{\partial}{\partial t}\left[m(x)\frac{\partial v}{\partial t}\right] + \frac{\partial}{\partial t}\left[2mc_0\frac{\partial v}{\partial x}\right] + \frac{\partial}{\partial x}\left[mc_0{}^2\frac{\partial v}{\partial x}\right]$$

$$\frac{\partial}{\partial x}\left[\mathrm{P}(x)\frac{\partial u}{\partial x} + \mathrm{EA}(x)\left(\frac{\partial u}{\partial x} + \left(\frac{dy}{dx}\right)\frac{\partial v}{\partial x}\right)\right] = \frac{\partial}{\partial t}\left[m(x)\frac{\partial u}{\partial t}\right] + \frac{\partial}{\partial t}\left[2mc_0\frac{\partial u}{\partial x}\right] + \frac{\partial}{\partial x}\left[mc_0{}^2\frac{\partial u}{\partial x}\right] \tag{18}$$

where P(x) is the tension force, E(x) is the Young's modulus, A(x) is cross sectional area, m(x) is the mass per unit length, and c_0 is the moving velocity of the cable's rigid body motion. Symbols u and v stand for the displacements in the horizontal (x) and vertical (y) axes, respectively.

For a uniform cable under the action of a constant tension force, the governing differential equations in the frequency domain can be derived as

$$\frac{\partial}{\partial x}\left\{\left[P - mc_0{}^2 + EA(y')^2\right]\frac{dv}{dx} + \left[EAy'\right]\frac{du}{dx}\right\} = -m\omega^2 v + 2i\omega mc_0\frac{dv}{dx} \tag{19a}$$

$$\frac{\partial}{\partial x}\left\{\left[P - mc_0{}^2 + EA\right]\frac{du}{dx} + \left[EAy'\right]\frac{dv}{dx}\right\} = -m\omega^2 u + 2i\omega mc_0\frac{du}{dx} \tag{19b}$$

Assume the profile of the cable can be approximated by a straight line with a slope y' and a zero curvature ($y'' = 0$), the system of equations in the frequency domain can be further simplified as

$$\begin{bmatrix} \overline{\lambda}^2 EAy' & \overline{\lambda}^2\left[P + EA(y')^2\right] + m\overline{\omega}^2 \\ \overline{\lambda}^2\left[P + EA\right] + m\overline{\omega}^2 & \overline{\lambda}^2 EAy' \end{bmatrix}\begin{Bmatrix} u \\ v \end{Bmatrix} = \begin{Bmatrix} 0 \\ 0 \end{Bmatrix} \tag{20}$$

in which $\overline{\omega} = \omega - ic_0\overline{\lambda}$, and $\overline{\lambda}$ is the complex spectral constant.

The corresponding spectral equation is then in a form as

$$\left(\overline{\lambda}^2 EAy'\right)^2 - \left\{\overline{\lambda}^2\left[P + EA(y')^2\right] + m\overline{\omega}^2\right\}\left\{\left[\overline{\lambda}^2(P + EA)\right] + m\overline{\omega}^2\right\} = 0 . \tag{21}$$

The two roots for $\overline{\omega}^2$ are

$$\overline{\omega_1}^2 = -\overline{\lambda}^2\left(\frac{P}{m}\right) \quad \text{and} \quad \overline{\omega_2}^2 = -\overline{\lambda}^2\left(\frac{P + EA\left(1 + y'^2\right)}{m}\right). \tag{22}$$

As a result, the phase and group velocities for the cable are expressed in the two constants, respectively, as

$$c_1 = \frac{\omega_1}{k} = \frac{\overline{\omega_1}}{k} - c_0 = \sqrt{\frac{P}{m}} - c_0 \tag{23}$$

and $$c_2 = \frac{\omega_2}{k} = \sqrt{\frac{P}{m} + \frac{EA\left(1 + y'^2\right)}{m}} - c_0 \tag{24}$$

where k, the imagery part of $\overline{\lambda}$, is the wave number.

Finally, the special case of a horizontal strand at fixed position with $y' = 0$ and $c_o = 0$ leads to two non-dispersive wave velocities as

$$c_1 = \sqrt{\frac{P}{m}} = \sqrt{\frac{\sigma_P A}{\rho A}} = \sqrt{\frac{\sigma_P}{\rho}} \tag{25}$$

$$c_2 = \sqrt{\frac{\sigma_P}{\rho} + \frac{E}{\rho}} = \sqrt{\frac{E}{\rho}\left(\varepsilon_P + 1\right)} \tag{26}$$

The former recovers the traveling velocity of the transverse wave of a tensioned cable while the latter shows a similar form as the wave velocity of an unconfined longitudinal wave along bars with a modification term due to the tension force.

3. Dispersion curves for prestressed members

In this section, all numerical results associated with the three 1-D member theories were computed assuming that the Poisson's ratio is 0.29. This particular value of the Poisson's ratio, appropriate for a steel member, allows the comparison between subsequent computed results and some well-known published data adopted in several textbooks and articles.

3.1. Longitudinal waves in rod

Based on the second order theory proposed by Mindlin and McNiven, dispersion curves associated with three vibration modes can be obtained accordingly with arbitrary values of the adjustment coefficients k_i. While the adjustment coefficients are mainly used to match the variation trends, discrepancies at the limiting velocities and cut-off frequencies of the dispersion curves for all three modes do exist in the current theory. For example, it appears that the approximation theory is incapable of matching all limiting values and varying trends simultaneously. Moreover, the limiting velocity for the third branch is not adjustable and thus always converging to an incorrect value, the P-wave velocity. The dispersion curve corresponding to the first mode however can agree very well with the 3-D solution over the entire frequency/wave number ranges as long as the adjustment coefficients

satisfies specific conditions derived from the exact theory, as illustrated by Mindlin and McNiven. Note that the first mode behavior is the most important phenomenon when studying the axial vibration due to a uniformly distributed excitation. Consequently, this second order theory serves as a very useful alternative to reproduce practical dispersion curves for the longitudinal wave propagation in rods.

Figure 1(a) shows the dispersion curves associated with the phase and group velocities for the first three modes of the longitudinal waves. The three phase curves, c_i, were directly computed from the so-called Pochhammer Eq. [10]. Three group curves c_{gi} were numerically evaluated from the phase velocities and the real part of the wave numbers using normal finite difference formulae. As can be seen from the figure, the first mode curves approach the Rayleigh wave velocity C_r and the higher order branches converge to the shear wave velocity C_s for very large wave number k. Only first mode curves reach a limiting velocity of the unconstrained bar velocity $c_b = (E/\rho)^{1/2}$ at the zero wave number.

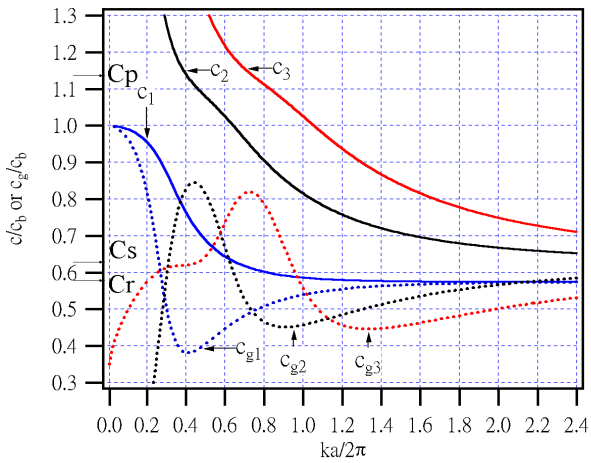

(a) Exact dispersion with ν=0.29

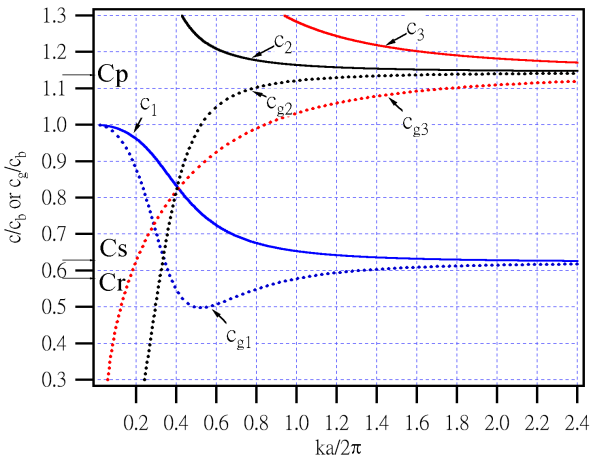

(b) Approximation dispersion with ki's =1.0

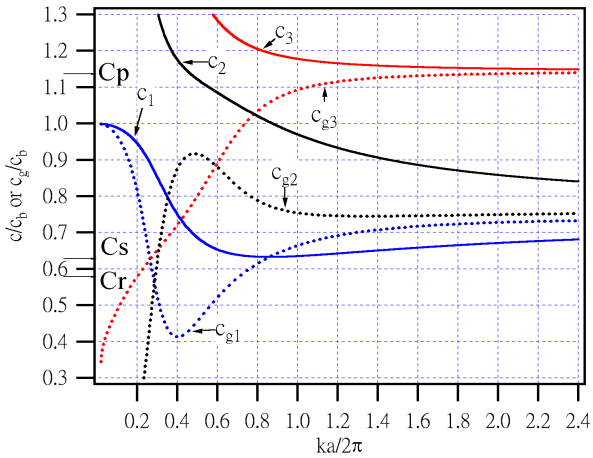

(c) Approximate dispersion with k_1=0.8794, k_2=1.1546

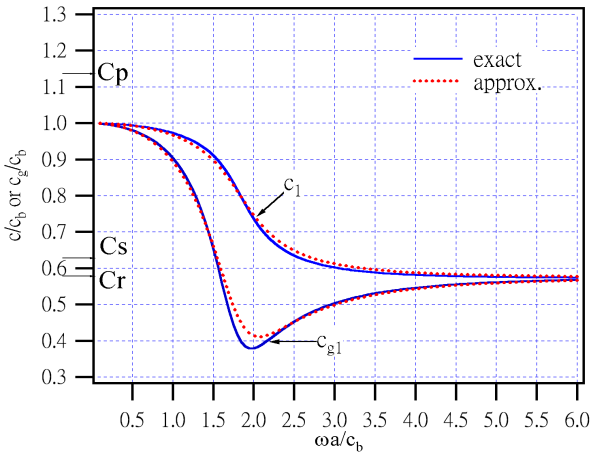

(d) Comparison between dispersion of 1st mode wave with k_1=0.965, k_2=1.0.

Figure 1. Exact and approximate dispersion curves of the first three modes for the longitudinal waves in a bar with circular cross section (k_3=1.1227k_1 and k_4=1.2785k_2 for (c) and (d)).

The approximate curves for the first three modes, based on the 1-D longitudinal theory as shown in figure 1(b), are obtained by assigning all adjustment coefficients to be unity. Except for the first-mode curves, the agreement between the exact and the approximate curves are poor. Instead of approaching Rayleigh and shear wave velocities, the approximate curves reach the shear and P-wave velocities respectively. To match the approximate curves with the exact ones within the region of small values of wave numbers, Mindlin and McNiven [2] proposed several formulae for the adjustment coefficients. Among them the expression in Eq. (27) ensures the match between the exact and approximate values at the zero wave number. Thus it is utilized in this paper when computing the approximate dispersion curves unless specified otherwise.

$$\left(\frac{k_2}{k_4}\right)^2 = \frac{\delta^2}{24}, \qquad \left(\frac{k_1}{k_3}\right)^2 = \frac{\eta^2\chi^2}{8(\eta^2-1)}, \qquad \eta^2 = \frac{2(1-\nu)}{(1-2\nu)} \tag{27a}$$

$$\eta^2\chi J_0(\chi)/J_1(\chi) = 2 \tag{27b}$$

In Eq. (27), δ and χ represent the first roots of $J_1(\delta) = 0$. J_0 and J_1 are the Bessel functions of the first kind of the zero and the first order, respectively. For Poisson's ratio of 0.29, Eq. (27) implies that $k_3 = 1.1227k_1$ and $k_4 = 1.2785k_2$.

The curves plotted using the ki values proposed by Mindlin and McNiven [2] are shown in figure 1(c), where the corresponding k_i for $\nu = 0.29$ are $k_1 = 0.8794$, $k_2 = 1.1546$, $k_3 = 0.9873$,and $k_4 = 1.4762$. By comparing with the exact curves in figure 1(a), the approximations in figure 1(c) are far better within the region of small wave numbers than that of large wave numbers. However, it is concluded from the parametric study in this work that the approximate dispersion curves associated with the first mode waves can be reasonably predicted based on various quadruplets of appropriately selected k_i. For example, figure 1(d) illustrates good agreement between the approximate and the exact curves for the first mode curves when choosing $k_1 = 0.965$, $k_2 = 1.0$, $k_3 = 1.1227k_1$, and $k_4 = 1.2785k_2$. For easier application of dispersion curves to practical cases, the curves in figure 1(d) and those appeared subsequently are plotted as functions of the dimensionless frequency, $\omega a/c_b$.

The effect of peripheral stresses on the dispersion curves of an axially loaded member can be determined using this approximate model. Only the longitudinal stress acting on a confined straight member will be considered in this section. Assuming the longitudinal stress is a function of the first-order axial displacement u, the parameter y_2 in Eq. (11) then becomes zero. The approximate dispersion curves predicted using this second order 1-D theory with peripheral stresses specified in Eq. (11) show apparent deviations from the original curves where the significant peripheral restraints are included. Figures 2(a) and 2(b) illustrate respectively the variation of dispersion curves associated with phase and group waves in which negative values of y_1 represent tension in the peripheral wires causing confined effects to the centered wire. The degree of restraints clearly affects the approximate dispersion curves. A value of $2.3G$ represents the spring constant which is generally utilized in a Soil Structure Interaction analysis to model the surrounding effect on the structural member due to the infinite (soil)

medium. A surrounding media of finite thickness, such as the thin peripheral wires, may results in insignificant restraining effect without the aid of significant confining stresses. On the other hand, large confining stresses caused by a huge prestressing force may lead to a significant restraining effect and thus a relatively large stiffness constant for the distributed springs in the analysis model.

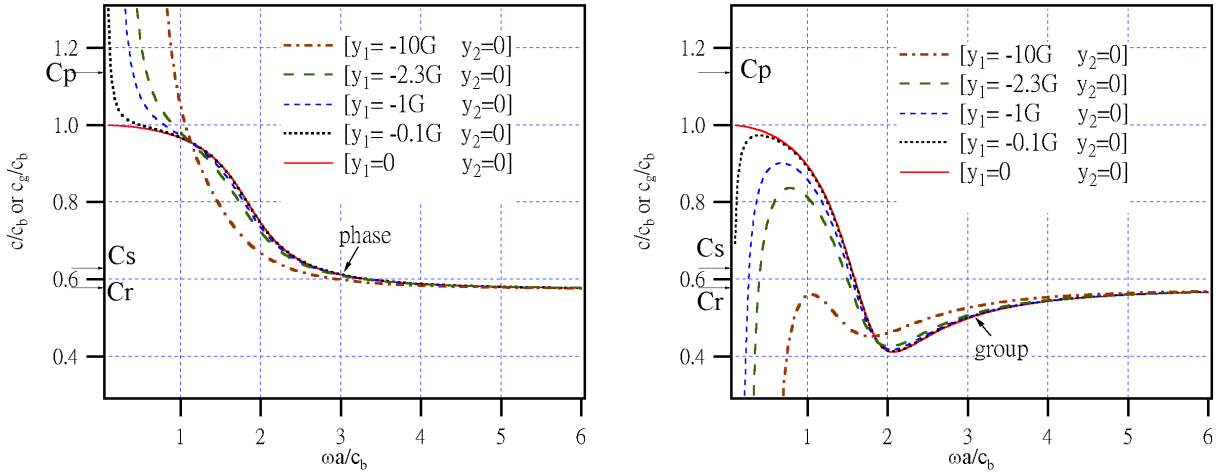

(a) Variation of dispersion for phase velocity (b) Variation of dispersion for group velocity

Figure 2. Effect of considering peripheral stresses on the predicted dispersion curves of the first mode (k_3=1.1227k_1 and k_4=1.2785k_2).

The existence of the distributed springs results in a cut-off frequency below which waves are evanescent instead of propagating, as can be observed in the low frequency region of figure 2(b). In addition the phase velocity greatly increases within the range between the cut-off frequency and a frequency near C_p/a, while the group velocity significantly decreases for the same frequency range. For the higher frequency range, both phase and group velocities stay closely to the original restraint-free curves. It could be seen from figure (2) that low-frequency signals may be more appropriate than high-frequency signals to be used in distinguishing the pre-stressing force applied to the center wire.

Frequency-dependent coefficients for springs derived from the mechanics of a curved or helical member may be more suitable than the stiffness constant currently illustrated in modeling the confining effect caused by the peripheral wires. The intension of using the proposed 1-D theory to model the 7-wire strand is just to preliminarily evaluate the feasibility of its possible application to the related dispersion analysis. Given the finite diameter of the peripheral wires and their spiral configuration, more rigorous analyses would be required to further verify this preliminary conclusion.

3.2. Flexural waves in axially loaded beam

It is well recognized that, for the flexural wave propagation, Timoshenko-type theories result in very good approximations for the first two modes of flexural vibration in relation to the 3-D exact theory. Figure 3 shows the dispersion curves associated with a beam of circular cross section with or without the interaction of a tensioned axial force. It can be seen from figure 3(a) both phase and group velocities of the first mode waves approach the approximate Rayleigh wave velocity,

$(\kappa G/\rho)^{1/2} \approx C_r$, and those of the second mode waves approach the unconstraint longitudinal wave velocity, $c_b = (E/\rho)^{1/2}$, at the high frequency region. In addition the second mode curves exhibit a cut-off frequency at $\omega_{cut\text{-}off} = (\kappa GA/\rho I)^{1/2}$. Figure 3(b) shows as an example the dispersion curves with the consideration of the effect due to a tensioned axial force in which a relatively large force $N = 0.1EA$ is used to illustrate the effect. It is interesting to note that a tensioned axial force results in increases in both phase and group wave velocities for the first mode wave while the changes in the second mode wave are rather small and thus negligible. Another observation is that, for static and very low frequency cases, both phase and group velocities associated with cases with tensioned forces approach the transverse velocity of a simple cable wave, $C_t = (\sigma/\rho)^{1/2}$ with σ and ρ standing for the axial stress and mass density, respectively.

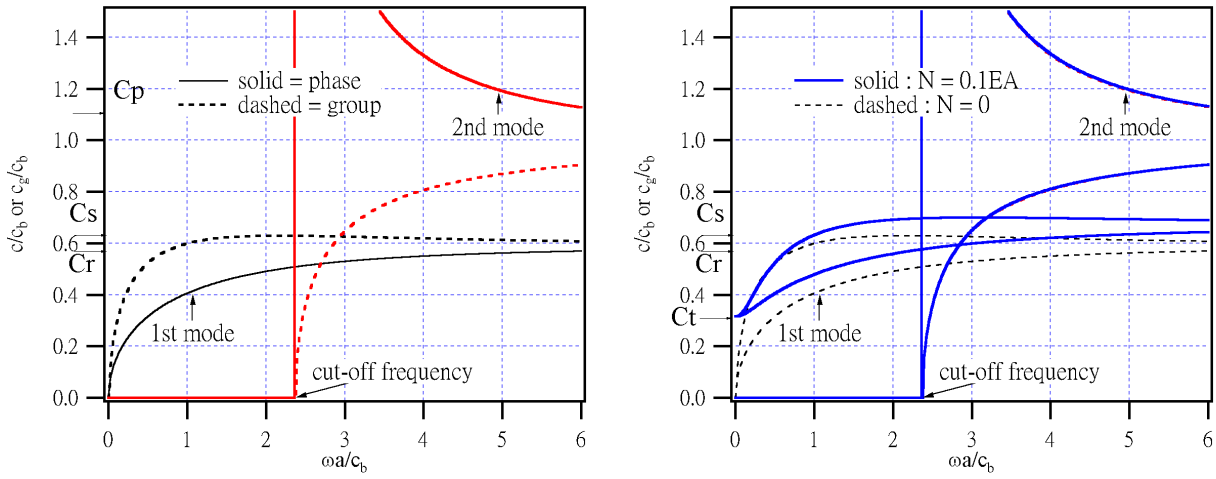

(a) dispersion curves for flexural members without axial force

(b) dispersion curves for flexural members with tensioned axial force N of $0.1EA$

Figure 3. Approximate dispersion curves for the first two modes of flexural waves (shear coefficient κ = 0.9, Poisson's ratio ν = 0.29).

Concerning the potential application of such dispersion relation to the NDT evaluation of steel members, the axial force shown in figure 3(b) is too high to be realistic. To gain a better understanding in the effect of tensile axial forces on the dispersion curves, figure 4(a) summarizes three pairs of curves associated with typical levels of prestressing forces for grade 270 strands, namely forces due to the axial strains of 0.5%, 0.7% and 1.0%. The axial strains of the last two levels are intended to characterize realistic strain rates corresponding to the stresses at the elastic limit and at yielding in which the yielding stress was assumed being deducted of 15% from its elastic value. Thus the axial force level for the 1% strain is designated as 0.0085 EA as shown in figure 4. The phase velocity increases as the tensile stress increases while the group velocity does the opposite except for the very low frequency region. However, the deviation between these curves and the original curves without axial force seems unclear. To have a better quantitative index in rating the effect of the loading levels on the wave velocities, the relative percentage of deviation of the curves in relation to the original one for the three tensile cases are computed and plotted in figures 4(b) and 4(c).

It is clear that the difference between cases of different loading levels is more significant

in the low frequency region than that in the higher frequency region. Waves of relatively low frequencies are more suitable than those of higher ones in detecting the loading level of the axially loaded members. It is also noted that the deviation shown in the dispersion curves of the group velocity is not as apparent as that for the phase velocity. Consequently, the phase velocity is the appropriate quantity to be utilized in the analysis task.

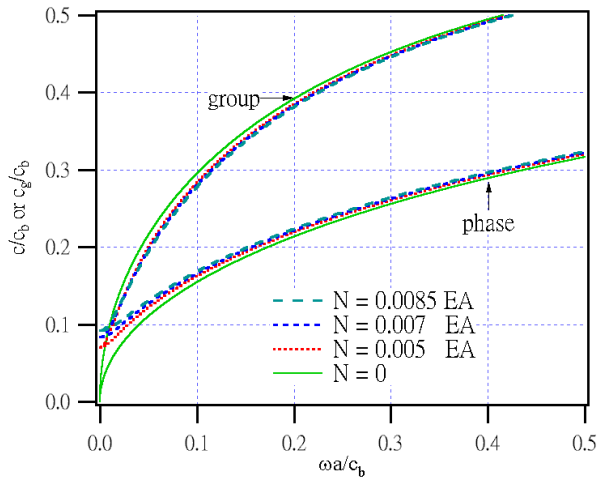

(a) Dispersion curves for flexural members under various levels of tension forces.

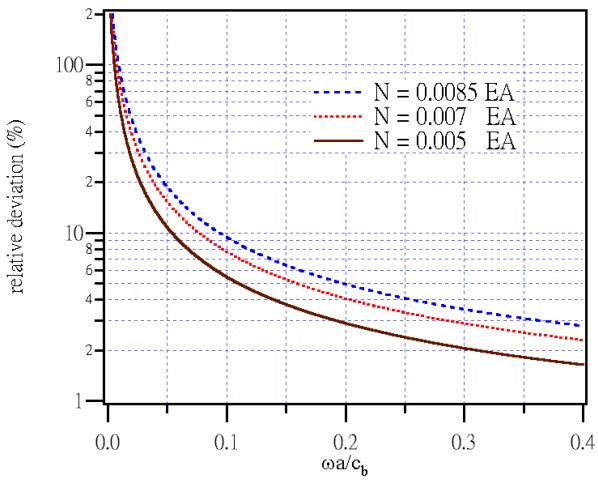

(b) Relative deviation in phase wave velocity caused by various tension forces.

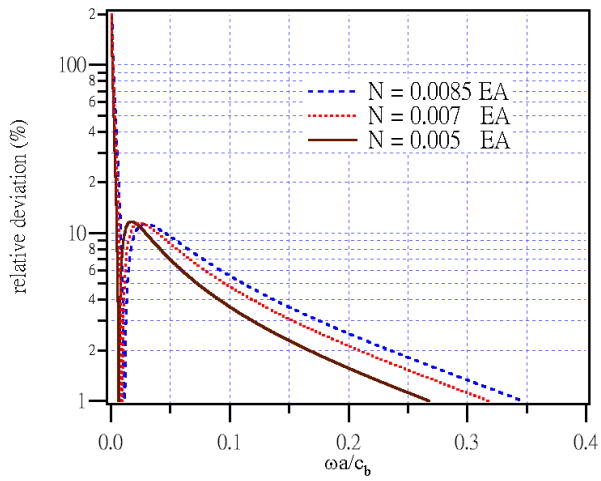

(c) Relative deviation in group wave velocity caused by various tension forces

Figure 4. Effect of tension forces on dispersion (shear coefficient $\kappa = 0.9$, $\nu = 0.29$).

3.3. Wave propagation in a tensioned cable

Based on Eqs. (25) and (26), the wave velocities associated with a tensioned cable are non-dispersive. The transverse wave velocity is identical to the cable wave velocity derived direction when no axial force is present is actually consistent with the unconstrained from

the traditional simple cable mechanics. The longitudinal wave velocity in the axial longitudinal velocity of bars. The tensile force results in increases only in the longitudinal wave velocity but not in the transverse wave velocity.

Owing to the various simplifications employed in deriving the dispersion relation, the cable model seems not as rigorous as the other two 1-D models. The second order rod theory is incapable of recovering or verifying the second wave velocity predicted by the cable model in which it is found that the increase in the prestressing stresses leads to a slight gain in the wave velocity of the longitudinal vibration. However, the simple non-dispersive wave velocities correspond well with the near-static phase velocities of the first modes associated with the transverse and longitudinal vibrations.

4. Numerical example for a straight wire subjected to tension force

In this section, a 7-wire strand of grade 270 with nominal diameter 12.7 mm, nominal area 98.7 mm^2 is used to illustrate the application of the approximate dispersion curves to the prediction of dynamic characteristics associated with vibration and wave propagation of various frequency ranges. Young's modulus, Poisson's ratio and mass density of the wire are 200×10^9 N/m^2, 0.29 and 7845 kg/m^3, respectively. Based on the dispersion curves derived in the previous section, the longitudinal waves were analyzed for the center wire assuming its nominal area is 1/7 of the cross sectional nominal area, while the transverse waves were investigated for the entire strand providing the cross sectional properties are uniform. With these assumptions, the propagation velocities C_p, c_b, C_s, C_r are about 5800, 5050, 3150, 2900 m/s, respectively, and the equivalent radii for a single wire and the entire 7-wire strand are about 2.1 mm and 5.6 mm.

Example 1 : longitudinal waves in center wire

According to figure 2, the appropriate frequency range for distinguishing the prestressing effects starts approximately from a dimensionless frequency of C_p/a to $2C_p/a$. Consequently, it can be predicted that a banded signal with its center frequency near 440 kHz and most of its energy within 1 MHz may result in optimal experimental responses for an NDT test. On the other hand, the wave velocities remain constantly approaching C_r regardless of the prestressing level. As a result, high frequency signals consisting of mostly the first mode waves can lead to the steadiest outcomes for signal analyses involving traveling times of waves. It should also be noted that the propagation velocity of very high frequency signals, for instance frequency higher than 2 MHz, is the Rayleigh wave velocity instead of the longitudinal velocities C_p or c_b. The level of prestressing may also be recovered from detecting the cut-off frequency of the first mode. However, we feel that this preliminary conclusion requires more investigation because that the currently employed spring constant is too simple to reflect the complex features of the multiple reflections from the outer edges of the 6 spiral wires. Further studies are needed in order to draw more realistic conclusions regarding the cut-off frequency indication.

Example 2 : Flexural waves in 7-wire strand

As in the longitudinal case, figure 3 shows that the prestressing effect on the dispersion relation can be distinguishable at the low frequency region but is not so clear at the higher frequency region. Based on the deviation trends illustrated in figure 4, the elastic dispersion analysis at the low frequency range seems potentially useful in extracting the information regarding the total axial force in a strand. The first possible method is to determine the wave velocity at near zero frequency which can reveal the magnitude of the tension force since the wave velocity is equal to $C_t = (\sigma/\rho)^{1/2}$ as discussed in the previous section.

The near static wave velocities C_t for the two loading cases within elastic limit, 0.005EA and 0.007EA, are about 0.071 c_b (=360 m/s) and 0.083 c_b (=420 m/s), respectively. Using 10% loss in the 0.7% prestressing case as an example, the near static wave velocity is about 0.080 c_b (=400 m/s) which implies a difference from the original value of about 5%. The difference is not very apparent but seems to be detectable from a practical point of view.

For cases with the tensile force dramatically varied, the second possible way is to monitor changes in wave velocities at very low frequency region. Using figure 4(b) as an example, a change of stress state from 0.007 EA to 0.005 EA with a threshold for detectable changes of 5% indicates that the frequency range of interest may have to be within a dimensionless frequency $\omega a/c_b$ of about 0.05, which corresponds to a frequency around 7kHz. However, when considering the stress state beyond the yielding stress, the above example may not be as useful as it appears for the following reasons. First, the phenomenon of the inelastic wave propagation may not be reasonably recovered by the elastic dispersion curves. Secondly, even if the elastic dispersion still provide useful correlation with the inelastic dispersion, the post-yielding behavior of the strand causes relatively little difference in stress when comparing to the corresponding change in strain. As a result, the deviation in the dispersion relation may be too imprecise to be decided.

Finally, It is worth of noting that the effect of different levels of axial forces on nonlinear wave propagation in a rod can be studied from the classical Pochhammer equation with the so-called Murnagham's third order elastic constants as done by Chen & He [11]. However, such exact solution may not be capable of correctly predicting the inelastic dispersion for the 7-wire strand due to the complex geometry of wires. Moreover, the counter part solution for the nonlinear transverse waves appears to be very difficult. It was never derived to the best knowledge of the authors.

5. Conclusions

In this paper the theoretical background for several rigorous 1-D member theories was first summarized and then dispersion curves for longitudinal and transverse waves were computed and plotted in terms of dimensionless parameters. To demonstrate the use of these approximate dispersion curves in predicting the axial force of a linear member, a couple of casestudies associated with both the longitudinal and transverse wave propagations in a 7-wire strand were carried out. From the numerical results obtained at current stage, the application of these rigorous 1-D theories to evaluate the dispersion characteristics for prestressed member is optimistic within the elastic limit.

Regarding the approximation of longitudinal wave propagation in rods, the use of the 3-mode Mindlin-McNiven theory with appropriate adjustment coefficients only guarantees good agreement for the low wave number/frequency region. Arrangement can be made to match the exact solutions for the entire frequency region for the first-mode waves. Therefore, it should always keep in mind that the prediction using such theory is good only when the first mode motion is the dominant one for the dynamic problem of interest.

In deriving the dispersion formulae for the center wire of a strand, some special modifications with respect to the peripheral stresses were taken into account such that the possible effect due to prestressing force can be reasonably recovered. The factor currently considered is the correlation of the peripheral forces with the displacement functions via a simple spring constant. Further considerations may include more rigorous frequency-dependent formulae derived from mechanics of curved members in replacing the simple constant and may also include distributed restraints in the radial direction. In other words,

the current results indicate that the potential of using the 3-mode 1-D theory is optimistic but these results need to be further verified numerically or even experimentally. Although the beam model for the center wire is not discussed in this paper, additional consideration of the peripheral stresses as the distributed springs can be easily incorporated into the proposed beam theory, as illustrated in the rod theory. Nevertheless, once reliable representations of the confining effects due to peripheral wires are available, these improved models will enhance the application of rigorous 1-D theories to the dispersion studies associated with the prestressing strand.

From the studies on the transverse wave propagation for the strand, it was found that the near-static wave velocity reflects pretty well the level of axial stresses. Therefore, the degree of prestressing may also be determined from measuring the transverse dispersion in the low frequency region.

Two non-dispersive wave velocities recovered by the cable model proposed by Sarkar & Manohar seem not as realistic as those predicted by the other two 1-D theories. The simple form may be resulted from several assumptions made during the linearization of the nonlinear differential equations. It should be noted that such model was reported being very useful in modeling the dynamics of sagged cables as illustrated in reference [7].

All the dispersion relations of the 1-D models in this paper have been obtained assuming members remain elastic behavior. Non-linearity due to strain-displacement relationships and constitutive equations are not considered. Such nonlinear effects can be dealt with by incorporating certain higher order parameters in the Pochhammer equation for cases associated the longitudinal wave. However, the application of this type of exact analysis may not be possible for a 7-wire strand. Further investigations regarding both theoretical and experimental aspects of this topic are still required in order to draw a comprehensive set of concluding remarks.

The 1-D approximation theories provide simpler alternatives in modeling certain complicated elasticity problems. The major advantage of using an appropriate 1-D formulation in the wave propagation analysis of slender members, even when exact formulations exist, is that the computation of dispersion curves can be minimized without sacrificing the accuracy of the solution as long as the structural response remains elastic. This is especially true for parametric studies related to dynamic problems involving non-destructive testing and (NDT) evaluation as illustrated by the authors [8]. Owing to the fact that the distributed properties can be easily taken into account by the summarized formulations in this work, this type of 1-D formulation is particularly useful for dynamic analyses involving grouted tendons, embedded piles, and immersed members taking into account fluid structure interaction.

Acknowledgements

The authors thank the National Science Council of Taiwan, for the financial support through the Grants NSC 89-TPC-7-324-002 and NSC 89-2211-E-324-033.

Appendix notations

a = radius of a circular rod

A = cross sectional area

c_0 = rigid body velocity of cable

c_1 , c_2 , c_3 , c_{g1} , c_{g2} , c_{g3} = phase and group wave velocities for the 1st 3 modes

C_p , C_s , C_r , c_b = P, S, Rayleigh, and unconstrained bar wave velocities

D_i's = specific frequency inertances

E = Young's modulus

ε_p , σ_p = axial strain and stress in cable due to tension force

F , F_1 = first order (uniform) and second order axial forces

G = shear modulus

I = moment of inertia

I_p = polar moment of inertia

J_0 , J_1 = Bessel functions of the 1st kind of the zero and 1st order

k = wave number

k_i = adjustment factors for Mindlin and McNiven rod theory

κ = shear coefficient

λ , μ = Lame's constants

$\bar{\lambda}$ = spectral constants for cable theory

m = mass per unit length for cable

N = axial force in beam column

ν = Poisson's ratio

P = tension force in cable

P_r = internal force in radial direction

Q = lateral contraction moment

r , $\bar{r}$ = spectral constants

R , Z = peripheral stresses

ρ = mass density

u_1 , u = uniform axial displacements

u_c , ψ = lateral contraction displacement and strain

u_2 , w = quadratic axial displacement function and displacement at neutral axis

ω = circular frequency

x , $\hat{x}$ = Fourier transform pair

References

[1] Mindlin, R. D. and Herrmann, G. 1951. A One-Dimensional Theory of Compressional Waves in An Elastic Rod. Proceedings of the First U.S. *National Congress of Applied Mechanics*: 187-191.

[2] Mindlin, R. D. and McNiven, H. D. 1960. Axially Symmetric Waves in Elastic Rods. *Journal of Applied Mechanics,* 27: 145-151.

[3] Chen, Y.-H. and Sheu, J.-T. 1993. Axial Loaded Damped Timoshenko Beam on Viscoelastic Foundation. *International Journal for Numerical Methods in Engineering*, 36: 1013-1027.

[4] Yu, C. P. and Roësset, J. M. 2001. Dynamic Analysis of Frames Using Continuous Dynamic Stiffness Matrix. *Tamkang Journal of Science and Engineering*, 4, 4: 37-45.

[5] Yu, C. P. 1995. "*Determination of Pile Lengths Using Flexural Waves*". *Report GR95-3,* Geotechnical Engineering Center, Civil Engineering Department, The University of Texas at Austin, U.S.A.

[6] Yu, C. P. 1996. "*Effect of Vertical Earthquake Components on Bridge Responses*". Doctoral Dissertation, University of Texas at Austin, U.S.A.

[7] Sarkar, A. and Manohar, C. S. 1996. Dynamic stiffness matrix of a general cable element. *Archive of Applied Mechanics*, 66: 315 – 325.

[8] Chiang, C. H., Yu, C. P., and Hsu, S. T. 2000. Assessment of Ungrouted Tendon and Measurement of Residual Stress Using NDT Methods. Presented in *the 27th Annual Review of Progress in Quantitative Nondestructive Evaluation (QNDE)*, Ames, Iowa, U.S.A., July 16th to July 21st, 2000.

[9] Press, W. Teukolsky, S., Vetterling, W., and Flannery, B. 1992. "*Numerical Recipes*", second Ed., Cambridge.

[10] Graff, K. 1975, "*Wave Motion in Elastic Solids*". Dover Publications, New York, U.S.A.

[11] Chen, H. L. and He, Y. 1992. An Ultrasonic Method for Stress Measurement of Prestressed Bars. *Vibro-Acoustic Characterization of Materials and Structures. ASME, NCA*, 14: 121 – 129.